Chemical Science

ROYAL SOCIETY OF CHEMISTRY

EDGE ARTICLE

View Article Online
View Journal | View Issue

Cite this: *Chem. Sci.*, 2020, **11**, 9884

All publication charges for this article have been paid for by the Royal Society of Chemistry

Received 15th July 2020
Accepted 24th August 2020

DOI: 10.1039/d0sc03858j

rsc.li/chemical-science

Effects of ruthenium hydride species on primary amine synthesis by direct amination of alcohols over a heterogeneous Ru catalyst†

Yusuke Kita, [a] Midori Kuwabara,[a] Satoshi Yamadera,[a] Keigo Kamata [a] and Michikazu Hara *[ab]

Heterogeneously catalysed synthesis of primary amines by direct amination of alcohols with ammonia has long been an elusive goal. In contrast to reported Ru-based catalytic systems, we report that Ru–MgO/TiO_2 acts as an effective heterogeneous catalyst for the direct amination of a variety of alcohols to primary amines at low temperatures of *ca.* 100 °C without the introduction of H_2 gas. The present system could be applied to a variety of alcohols and provides an efficient synthetic route for 2,5-bis(aminomethyl)furan (BAMF), an attention-getting biomonomer. The high catalytic performance can be rationalized by the reactivity tuning of Ru–H species using MgO. Spectroscopic measurements suggest that MgO enhances the reactivity of hydride species by electron donation from MgO to Ru.

Introduction

Primary amines are known as versatile building blocks due to their convenient use in different fields of synthetic chemistry and serve as synthons for pharmaceuticals, agricultural chemicals and polymers.[1] Thus, a variety of synthetic methods to produce primary amines have been developed including the alkylation of ammonia, and reduction of amides, nitriles and nitro compounds, in addition to special methods (*e.g.*, Staudinger reduction and Hofmann degradation).[2] The direct substitution of alcohols with ammonia is considered to be the most rational synthetic protocol for primary amines because of the ready-availability of alcohols, and the low cost of ammonia, and it is attractive in terms of it being environmentally benign. Due to the low leaving-group ability of the hydroxy group, recent attempts have been devoted to the borrowing hydrogen (BH) methodology.[3] This system uses a powerful strategy that combines dehydrogenation, transformation of generated unsaturated compounds, and subsequent hydrogenation to form more complex molecules, without the need for tedious separation or isolation processes. Since the pioneering work with a Ru complex bearing a PNP pincer ligand by Gunanathan and Milstein,[4] some Ru- and Ir-based homogeneous catalysts have been developed for the selective synthesis of primary amines by the direct amination of alcohols with ammonia.[5] In view of the advantages of heterogeneous catalysts, such as ease of recovery, reusability, and stability, there is a substantial need for the development of efficient heterogeneous catalysts that enable selective conversion of alcohols into amines under mild reaction conditions for the environmentally benign production of chemicals. Although some Ni-based heterogeneous catalysts have been developed,[6] these systems require severe reaction conditions (Scheme 1 and Table S1†). Ru-, Co- and Pt-based catalysts are also active for the direct amination of alcohols;[7–9] however, these catalysts require molecular hydrogen, which is not required in principle. Besides the possible explanation for H_2 effects (regeneration of the active metal surface and the removal of coke),[7a,b] we propose that additional H_2 prevents H_2-release from the metal hydride species generated through the dehydrogenation of alcohols. Therefore, we have envisioned that electronic tuning of the ruthenium hydride species would

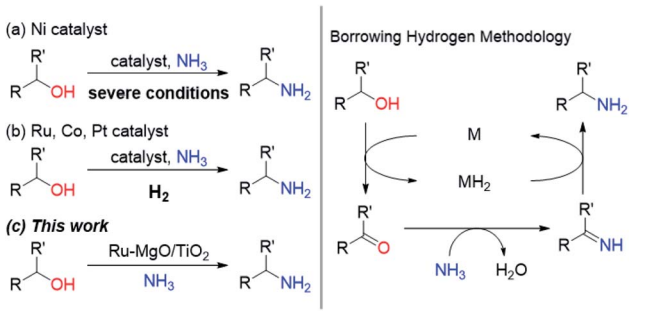

Scheme 1 Selective synthesis of primary amines by direct amination of alcohols and ammonia over heterogeneous catalysts through borrowing hydrogen methodology.

[a]*Laboratory for Materials and Structures Institute of Innovative Research, Tokyo Institute of Technology, 4259 Nagatsuta-cho, Midori-ku, Yokohama 226-8503, Japan. E-mail: hara.m.ae@m.titech.ac.jp*

[b]*Advanced Low Carbon Technology Research and Development Program (ALCA), Japan Science and Technology Agency (JST), 4-1-8 Honcho, Kawaguchi 332-0012, Japan*

† Electronic supplementary information (ESI) available. See DOI: 10.1039/d0sc03858j

result in the development of efficient catalysts for the direct amination of alcohols through a BH strategy. Despite the importance of metal hydride species in many hydrogen-involving reactions, the characterization of metal hydride species is still a challenge for heterogeneous catalysts.[10] We have focused on a basic support that can sufficiently stabilize Ru hydride species enough to require hydrogen acceptors for the dehydrogenative oxidation of alcohols catalysed by a supported Ru catalyst.[11] In this study, we report a supported Ru catalyst for basic oxide-enabled direct amination of alcohols with ammonia under mild reaction conditions without molecular hydrogen as an accelerator.

Results and discussion

The research began with the direct amination of furfuryl alcohol (**1a**) using Ru catalysts supported on simple basic metal oxides and hydroxides (Table S2†). Ru/MgO gave the desired primary amine in 77% yield; however, this catalyst could not be reused even after reduction treatment. To achieve more active and stable catalysts, we examined the deposition of Ru and Mg on high-surface-area supports. A Ru and alkaline earth metal co-deposited metal oxide supported catalyst (Ru–*x*M/support; *x* = M loading (wt%)) was prepared through the sequential deposition of Ru and an alkaline earth metal on the support by the wet-impregnation method. X-ray diffraction (XRD) analysis was conducted for Ru–20MgO/TiO_2 before and after hydrogen reduction (Fig. 1). $Mg(OH)_2$ was observed in addition to the TiO_2 (anatase) support before reduction. Reduction treatment of the sample resulted in the formation of MgO. We estimated the average size of MgO nanoparticles on TiO_2 from the XRD patterns. The grain size of MgO in Ru–MgO/TiO_2 estimated from the (200) diffraction lines using Scherrer's equation was 25 nm. This value is good agreement with the particle size 20–50 nm measured from the field-emission scanning electron microscope (FE-SEM) images of Ru–20MgO/TiO_2 (Fig. S1†). Peaks of the Ru species were not observed in the XRD patterns, possibly due to the high dispersion of the Ru species on the support. Transmission electron microscopy-energy dispersive X-ray spectroscopy (TEM-EDS) analysis of Ru–MgO/TiO_2 indicated that Ru and Mg were highly dispersed on the TiO_2 support (Fig. 2). To obtain information on the environment around Ru particles, the electronic states of Ru particles were examined with CO- adsorption infrared (IR) spectroscopy measurements (Fig. 3). The bands assignable to the stretching vibration of CO adsorbed on Ru can be shifted by the electron-donating character of the Ru particles.[12] A broad band (2038 cm^{-1}) with a shoulder (1925 cm^{-1}) was observed in the spectrum for Ru–20MgO/TiO_2, and these features were assigned to linearly adsorbed CO on partially oxidized Ru and CO bridged between two metallic Ru atoms, respectively.[13] X-ray photoelectron spectroscopy (XPS) measurements for Ru 3d of the catalyst showed that Ru^0 coexists with Ru^{4+} (Fig. S2†), which was consistent with the Fourier transform infrared spectroscopy (FT-IR) results. For Ru/TiO_2, both bands appeared at higher wavenumber positions (2056 and 1981 cm^{-1}), which indicated that Ru on Ru–20MgO/TiO_2 has higher electron-donating capability than Ru on Ru/TiO_2. Fig. 3 also shows that there is no significant difference in the band position between Ru–MgO/TiO_2 and Ru/MgO, which suggests that Ru is in contact with MgO rather than TiO_2 on Ru–MgO/TiO_2, and the electron donation from MgO, a strong electron-donating material, to Ru enhances the electron-donating capability of Ru on Ru–MgO/TiO_2. We measured amounts of acid and base sites of Ru–20MgO/TiO_2 and Ru/TiO_2 by pyridine-adsorbed IR

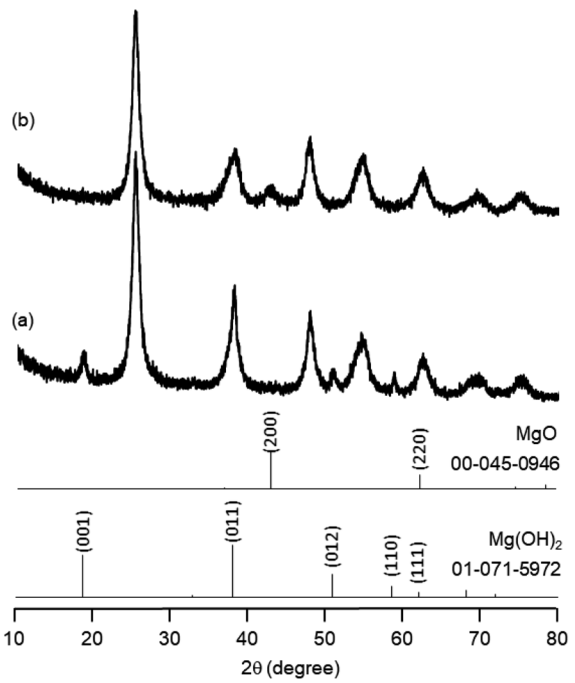

Fig. 1 XRD patterns for Ru–20MgO/TiO_2 before and after reduction.

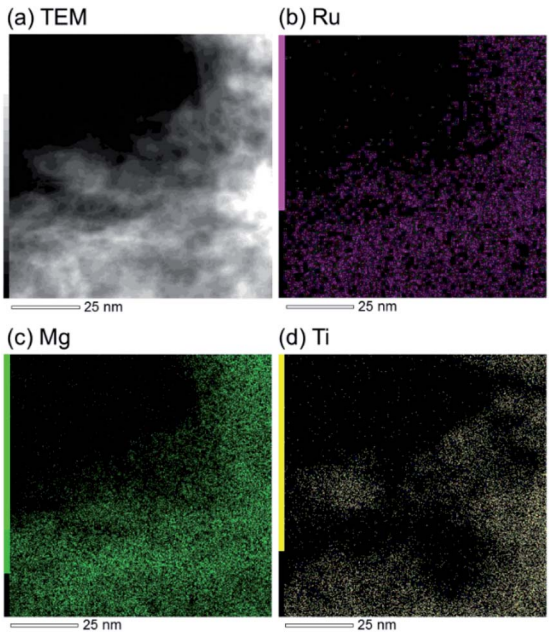

Fig. 2 TEM-EDS analysis of Ru–20MgO/TiO_2.

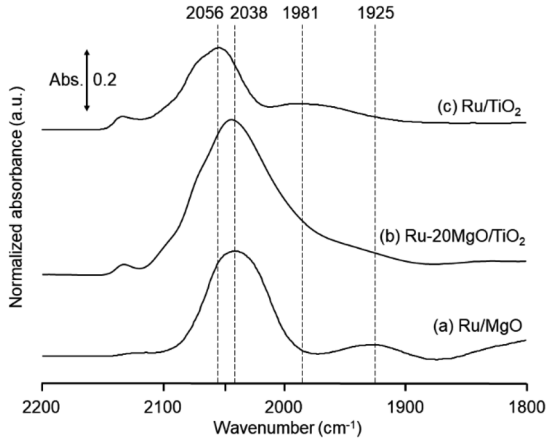

Fig. 3 Difference IR spectra of CO-adsorbed Ru/MgO, Ru–20MgO/TiO_2, and Ru/TiO_2.

measurements and CO_2 temperature-programmed desorption (CO_2-TPD) (Table S4†). Ru–20MgO/TiO_2 possesses higher amounts of acid sites than Ru/TiO_2 probably due to the higher surface area of Ru–MgO/TiO_2. Although there was no significant difference in the amounts of base sites between Ru–MgO/TiO_2 and Ru/TiO_2, the CO_2 desorption peaks around 250 °C of Ru/TiO_2 shifted to higher temperatures (450–650 °C) in the case of Ru–MgO/TiO_2 (Fig. S3†). Thus, the basicity of Ru–MgO/TiO_2 would be stronger than that of Ru/TiO_2, which would result in the acceleration of the alcohol dehydrogenation step.

The prepared catalysts were evaluated with respect to the direct amination of **1a** with ammonia in toluene at 110 °C for 20 h (Table 1). Ru–20MgO/TiO_2 exhibited high catalytic performance to give furfurylamine (**2a**) in 85% yield with a trace amount of the imine **3a** (entry 1). No other side products were observed in the reaction mixture. The turnover frequency (TOF) value is calculated based on the Ru dispersion to be 0.6 h^{-1}. This value is lower than those of reported Ru catalysts (Table S1†) due to the low reaction temperature (110 °C for Ru– MgO/TiO_2 *vs.* 150–220 °C for Ru/C, Ru/SiO_2, Ru/Al_2O_3, and RuNPs); however, the reported Ru catalysts showed low selectivity to primary amines in contrast to the present Ru– MgO/TiO_2 system. The effect of the support was then examined (entries 4–7). Low yields of **2a** were observed for other oxide supports, such as SiO_2, Al_2O_3, ZrO_2, and Nb_2O_5. There was no correspondence between the activity and support features, such as acid/base sites and electron-donating character. Mg loading had a high impact on the catalytic activity of the Ru catalysts. The deposition of lower and higher amounts of MgO resulted in a decrease of the yield of **2a** (entries 8 and 9). Other alkaline earth metals were not effective for the direct amination of alcohol (entries 10–12). Ru/TiO_2 also exhibited catalytic activity; however, only a 38% yield of **2a** was obtained (entry 13). In addition, the result of a physical mixture of Ru/TiO_2 and MgO was similar to that of Ru/TiO_2 (entry 14), which indicates that direct interaction between Ru and Mg is essential in achieving high activity for the direct amination of alcohols. Ru/Nb_2O_5 was not effective for the direct amination although it acts as a highly active and selective

Table 1 Catalyst screening[a]

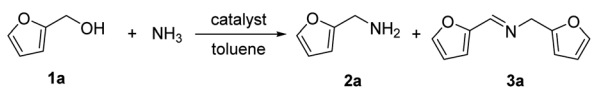

Entry	Catalyst	Conv. (%)	Yield (%) 2a	3a
1	Ru–20MgO/TiO_2	96	85	Trace
2[b]	Ru–20MgO/TiO_2	18	0	0
3[c]	Ru–20MgO/TiO_2	>99	94	0
4	Ru–20MgO/SiO_2	99	32	0
5	Ru–20MgO/Al_2O_3	99	59	0
6	Ru–20MgO/ZrO_2	76	24	0
7	Ru–20MgO/Nb_2O_5	43	17	0
8	Ru–10MgO/TiO_2	82	42	0
9	Ru–30MgO/TiO_2	87	52	0
10	Ru–20CaO/TiO_2	91	44	0
11	Ru–20SrO/TiO_2	79	58	0
12	Ru–20BaO/TiO_2	90	44	0
13	Ru/TiO_2	72	38	Trace
14	Ru/TiO_2 + MgO[d]	72	35	0
15[e]	Ru/Nb_2O_5	46	2	0

[a] Reaction conditions: catalyst (0.2 g), **1a** (0.5 mmol), pNH_3 (0.7 MPa), toluene (5 mL), 110 °C, and 20 h. Conversion and yield were determined by GC analysis. Yield (%) = product (mol)/initial **1a** (mol) × 100. [b] Operated in air. [c] 0.4 g catalyst was used. [d] 0.2 g Ru/TiO_2 and 0.04 g MgO were used as the catalyst. [e] Run at 180 °C.

catalyst for reductive amination (entry 15).[14] No reaction was observed when the reaction setup was assembled on a bench outside the glovebox (entry 2). After further optimization studies including solvent screening and the catalyst loading effect (Table S5†), the use of 0.4 g catalyst increased the yield of **2** to 94% (entry 3). Fig. 4 shows the results of the reuse experiment. After base treatment with NaOH and subsequent reduction with H_2 at 400 °C, Ru–20MgO/TiO_2 could be reused three times without loss of activity.

The present catalytic system could be applied to a variety of alcohols (Table 2). Electronic and steric effects were examined using substituted benzyl alcohol. The direct amination proceeded smoothly, regardless of the substituents at the para

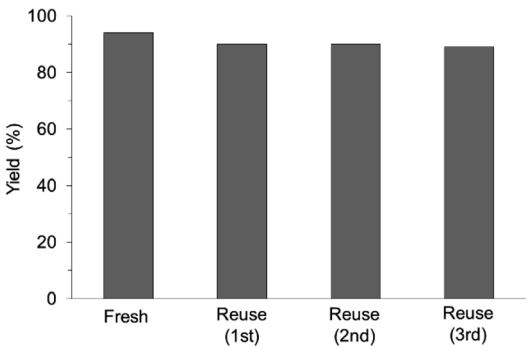

Fig. 4 Reuse experiments. Reaction conditions: Ru–20MgO/TiO_2 (0.4 g), **1a** (0.5 mmol), toluene (5 mL), pNH_3 (0.7 MPa), 110 °C, and 20 h.

Table 2 Substrate scope[a]

Entry	Substrate	Product	Yield (%)
1[b]	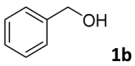 1b	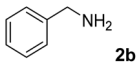 2b	91
2	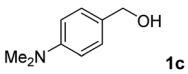 1c	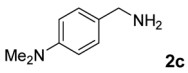 2c	82
3[c]	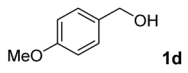 1d	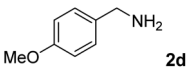 2d	89
4	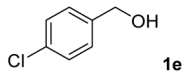 1e	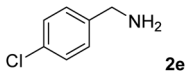 2e	72
5	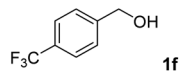 1f	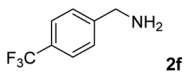 2f	76
6	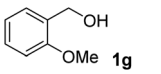 1g	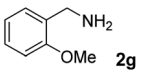 2g	81
7	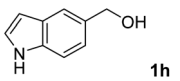 1h	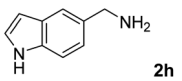 2h	67
8	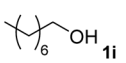 1i	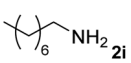 2i	78
9	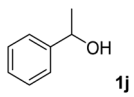 1j	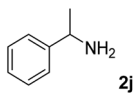 2j	61
10	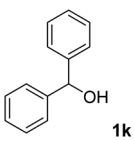 1k	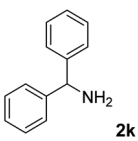 2k	67
11	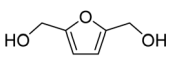 1l	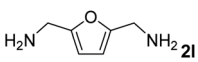 2l	86

[a] Reaction conditions: Ru–20MgO/TiO_2 (0.2 g), **1** (0.5 mmol), pNH_3 (0.7 MPa), toluene (5 mL), 110 °C, and 20 h. [b] Run at 100 °C. [c] Run for 30 h.

position, to give the corresponding primary amines in good to excellent yields (entries 2–5). A sterically hindered substrate is also applicable with this catalytic system (entry 6). In addition, the catalytic system has high functional group tolerance. The chloro group and indole skeleton remained intact during the reaction. The present Ru system could be applied to not only benzyl alcohol derivatives, but also to linear alkyl alcohols (entry 8). Secondary alcohols are also good substrates for direct amination with this catalyst system (entries 9 and 10). The product was obtained in moderate yield due to the formation of dehydroxylated products. Finally, the catalytic system was applied to the synthesis of 2,5-bis(aminomethyl)furan (BAMF), which is known as a biomonomer for polyamides and a hardener for epoxy resins.[15] When 2,5-bis(hydroxymethyl)furan (BHMF) was used as a substrate, the desired BAMF was obtained in 86% yield (entry 11). Compared with the reported methods for the synthesis of BAMF,[16] the present system has superiority in that a high yield of BAMF is produced under mild reaction conditions.

To determine whether the reaction proceeds through the BH strategy or not, we examined the hydrogenation of benzylidene aniline (**4**) with **1a** as a hydride source. As expected, hydrogenated product **5** was obtained in 27% yield along with the formation of furfural derivative **6** in 48% yield (Scheme 2a). **6** was generated through the formation of furfural by the dehydrogenation of **1a** and subsequent condensation with aniline derived from the hydrolysis of **4**. In addition, deuterium labelling experiments were conducted for the direct amination of benzyl alcohol-α,α-d_2 (**1b-*d*$_2$**) and subsequent acetylation with acetyl chloride (AcCl) to precisely calculate the deuterium content using ^{1}H nuclear magnetic resonance spectroscopy (NMR) (Scheme 2b). The deuterium content at the benzylic position in **8** was decreased to 39% from 98%. The decrease of the deuterium content suggests that the dehydrogenation of alcohols is reversible under the direct amination conditions. The source of the hydrogen is a hydroxide group or H_2O adsorbed on the catalyst surface. The deuterium content was also decreased when **1b-*d*$_2$** was exposed to the direct amination conditions without ammonia (Scheme 2c). No detection of the dehydrogenated product indicates that Ru–20MgO/TiO_2 can prevent H_2 release from the Ru hydride species, in contrast to Ru/TiO_2 which is known to be active for the dehydrogenation of alcohols under oxidant-free conditions.[17] In addition, the H_2-TPD analysis was carried out to evaluate the nature of the H species (Fig. S4†). The desorption peak at around 500 °C exclusively appears in the profile of Ru–20MgO/TiO_2. This peak is likely assignable to the desorption of spillover hydrogen on the support.[18] These results indicate that MgO promotes the hydrogen spillover, contributing to maintenance of H species in

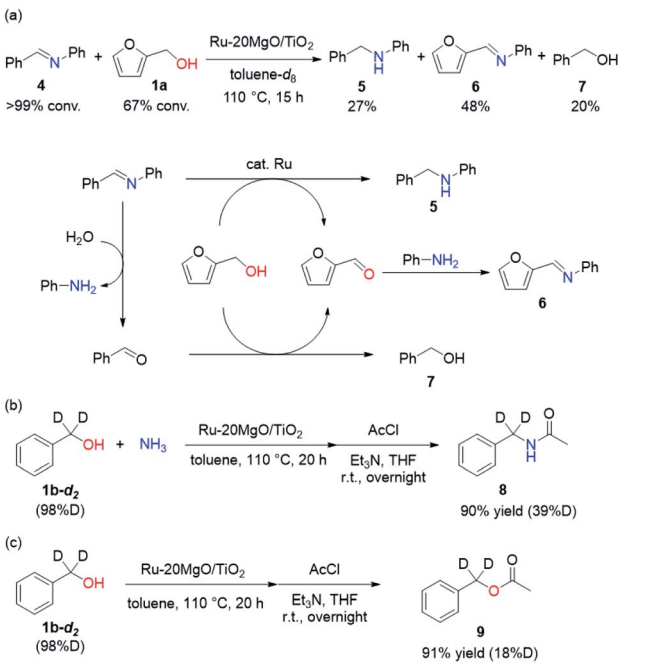

Scheme 2 Control experiments: (a) hydrogenation of benzylidene aniline (**4**) using furfuryl alcohol as a hydride source. (b) Direct amination of **1b-*d*$_2$**. (c) Exposure of **1b-*d*$_2$** to direct amination conditions without ammonia.

the vicinity of Ru particles. The dehydrogenation of alcohols was also confirmed using IR measurements with adsorbed isopropanol. As the temperature increased after the introduction of isopropanol to the IR cell, two bands were observed at 1733 and 1946 cm^{-1} (Fig. 3 and S6†). The band at 1733 cm^{-1} is assignable to the stretching vibration of C=O of gas phase acetone,[19] and that at 1946 cm^{-1} is due to the Ru–H species on Ru–MgO/TiO_2.[20] As a complementary result, Ru–D stretching vibration was observed at 1434 cm^{-1} from measurements using isopropanol-d_8 (Fig. S8†). When the hydrogen atom in Ru–H is replaced with a deuterium atom, the wavenumber for the Ru–H stretching vibration is expected to be shifted to 1441 cm^{-1}. The IR spectrum for the measurement using isopropanol-d_8 also showed a peak that was assigned to the Ru–H bond, which reflects the H/D exchange by reversible alcohol dehydrogenation. We cannot rule out the possibility that these peaks are assignable to the stretching vibrations of the C–D bond in acetone-d_6.[21] Comparison of Ru–MgO/TiO_2 with Ru/TiO_2 revealed that the band due to Ru–H on Ru/TiO_2 was at a higher wavenumber position (2006 cm^{-1}) than that on Ru–MgO/TiO_2 (Fig. 5). This difference indicates that the Ru–H bond is elongated due to the electron donation from MgO.

From the elongated Ru–H bond on Ru–MgO/TiO_2, hydrogenation ability can be differentiated by the effect of MgO. Therefore, the transfer hydrogenation of **4** was conducted over Ru–MgO/TiO_2 and Ru/TiO_2 (Fig. 6). When isopropanol is used as a hydride source, the MgO effect on the imine hydrogenation step can be discussed because the dehydrogenation of isopropanol is fast even at 60 °C as observed in IPA-adsorbed IR analysis (Fig. 5). As expected, hydrogenated product **5** was obtained in 81% yield for Ru–MgO/TiO_2 and in 60% yield for Ru/TiO_2. The higher hydrogenation ability of Ru–MgO/TiO_2 can be rationalized by the elongated Ru–H bond, as observed in isopropanol-probed IR measurements, which results in efficient direct amination under mild conditions.

Here we propose a mechanism for this reaction involving the dehydrogenation of alcohols (Scheme 3). Initially, the adsorption of an alcohol on the ruthenium surface forms a deprotonated alkoxide. An aldehyde is generated reversibly formed by β-hydride elimination from the Ru alkoxide. The concomitant Ru–H species, activated by MgO, hydrogenates the NH–imine derived from the aldehyde with ammonia to give the desired primary amines. The high activity of the Ru–H species resulted in high selectivity by the prevention of side reactions of imine intermediates. The lack of H_2 requirement could be attributed to the inhibition of Ru–H species decomposition through electronic tuning using MgO.

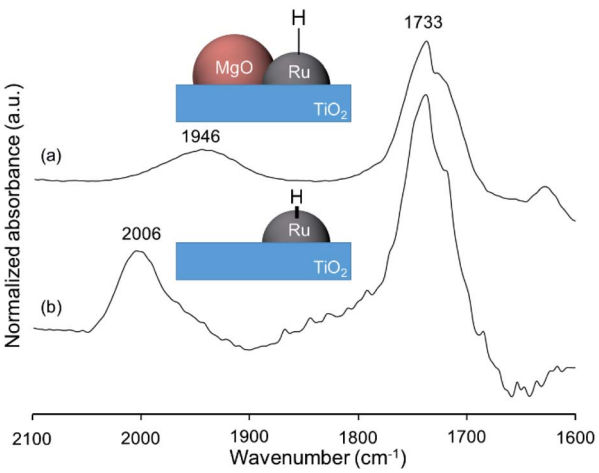

Fig. 5 Difference IR spectra of isopropanol-adsorbed (a) Ru–20MgO/TiO_2 and (b) Ru/TiO_2 at 60 °C.

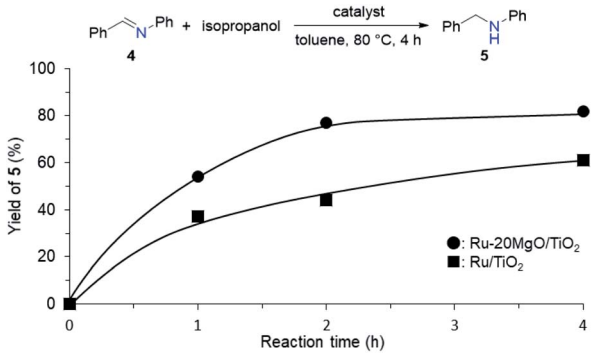

Fig. 6 Time courses for transfer hydrogenation of **4** over the supported Ru catalyst using isopropanol as a hydride source. Reaction conditions: catalyst (0.05 g), **4** (0.5 mmol), isopropanol (1 mL), toluene (4 mL), and 80 °C.

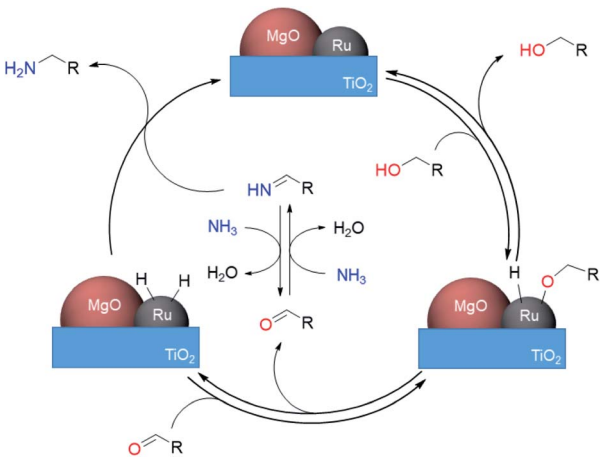

Scheme 3 Proposed reaction mechanism for direct amination of alcohols over Ru–20MgO/TiO_2.

Conclusions

We have demonstrated the direct amination of alcohols over Ru–20MgO/TiO_2. The direct amination of various alcohols proceeded efficiently to afford the desired primary amines in high yield. The present system is highly advantageous in that it requires no accelerator compared to reported Ru systems, and is reusable without loss of activity after the base treatment and reduction sequence. Direct amination catalysed by Ru–20MgO/TiO_2 proceeded through the BH methodology, as evidenced by

the formation of ruthenium hydride species from isopropanol. Mechanistic studies revealed that the effect of MgO can be (1) acceleration of the imine hydrogenation step by the electronic tuning of Ru particles, and (2) the anchoring effect that provides large dispersion and small particle size. These results with the metal hydride species are expected to provide a design guide for new heterogeneous catalysts for hydrogen-involving reactions.

Conflicts of interest

There are no conflicts to declare.

Acknowledgements

This work was financially supported by the Advanced Low Carbon Technology Research and Development Program (ALCA) of the Japan Science and Technology Agency (JST) (JPMJAL1205) and a fund from the Grants-in-Aid for Japan Society for the Promotion of Science (JSPS) Fellows and for Scientific Research from the Ministry of Education, Culture, Science, Sports, and Technology (MEXT) of Japan (18H05251).

Notes and references

1 (*a*) K. S. Hayes, *Appl. Catal. A: Gen.*, 2001, **221**, 187–195; (*b*) B. Chen, U. Dingerdissen, J. G. E. Krauter, H. G. J. L. Rotgerink, K. Möbus, D. J. Ostgard, P. Panster, T. H. Riermeier, S. Seebald, T. Tacke and H. Trauthwein, *Appl. Catal. A: Gen.*, 2005, **280**, 17–46; (*c*) I. Delidovich, P. J. C. Hausoul, L. Deng, R. Pfützenreuter, M. Rose and R. Palkovits, *Chem. Rev.*, 2016, **116**, 1540–1599; (*d*) A. Gandini, T. M. Lacerda, A. J. F. Carvalho and E. Trovatti, *Chem. Rev.*, 2016, **116**, 1637–1669.

2 K. Eller, E. Henkes, R. Rossbacher and H. Höke, *Ullmann's Encyclopedia of Industrial Chemistry*, Wiley-VCH, Weinheim, 2005.

3 (*a*) A. Corma, J. Navas and M. Sabater, *Chem. Rev.*, 2018, **118**, 1410–1459; (*b*) K.-i. Shimizu, *Catal. Sci. Technol.*, 2015, **5**, 1412–1427.

4 C. Gunanathan and D. Milstein, *Angew. Chem., Int. Ed.*, 2008, **47**, 8661–8664.

5 (*a*) S. Imm, S. Bähn, L. Neubert, H. Neumann and N. Beller, *Angew. Chem., Int. Ed.*, 2010, **49**, 8126–8129; (*b*) D. Pingen, C. Müller and D. Vogt, *Angew. Chem., Int. Ed.*, 2010, **49**, 8130–8133; (*c*) S. Imm, S. Bähn, M. Zhang, L. Neubert, H. Neumann, F. Lkasovsky, J. Pfeffer, T. Haas and M. Beller, *Angew. Chem., Int. Ed.*, 2011, **50**, 7599–7603; (*d*) M. Zhang, S. Imm, S. Bähn, H. Neumann and M. Beller, *Angew. Chem., Int. Ed.*, 2011, **50**, 11197–11201; (*e*) D. Pingen, O. Diebolt and D. Vogt, *ChemCatChem*, 2013, **5**, 2905–2912; (*f*) W. Baumann, A. Spannenberg, J. Pfeffer, T. Haas, A. Köckritz, A. Martin and J. Deutsch, *Chem.–Eur. J.*, 2013, **19**, 17702–17706; (*g*) D. Pingen, M. Lutz and D. Vogt, *Organometallics*, 2014, **33**, 1623–1629; (*h*) X. Ye, P. N. Plessow, M. K. Brinks, N. Schelwies, T. Schaub, F. Rominger, R. Paciello, M. Limbach and P. Hofmann, *J. Am. Chem. Soc.*, 2014, **136**, 5923–5929; (*i*) N. Nakagawa, E. J. Derrah, M. Schlwies, F. Rominger, O. Trapp and T. Schaub, *Dalton Trans.*, 2016, **45**, 6856–6865; (*j*) K.-i. Fujita, S. Furukawa, N. Morishima, M. Shimizu and R. Yamaguchi, *ChemCatChem*, 2018, **10**, 1993–1997.

6 (*a*) K.-i. Shimizu, K. Kon, W. Onodera, H. Yamazaki and J. N. Kondo, *ACS Catal.*, 2013, **3**, 112–117; (*b*) K.-i. Shimizu, S. Kanno, K. Kon, S. M. A. H. Siddiki, H. Tanaka and Y. Sakata, *Catal. Today*, 2014, **232**, 134–138; (*c*) Y. Liu, K. Zhou, H. Shu, H. Liu, J. Lou, D. Guo, Z. Wei and X. Li, *Catal. Sci. Technol.*, 2017, **7**, 4129–4135; (*d*) L. Ma, L. Yan, A.-H. Lu and Y. Ding, *RSC Adv.*, 2018, **8**, 8152–8163; (*e*) A. Tomer, Z. Yan, A. Ponchel and M. Pera-Titus, *J. Catal.*, 2017, **356**, 133–146; (*f*) A. Y. K. Leung, K. Hellgardt and K. K. M. Hii, *ACS Sustainable Chem. Eng.*, 2018, **6**, 5479–5484; (*g*) A. Tomer, B. T. Kusema, J.-F. Paul, C. Przybylki, E. Monflier, M. Pera-Titus and A. Ponchel, *J. Catal.*, 2018, **368**, 172–189; (*h*) Y. Liu, A. Afanasenko, S. Elangovan, Z. Sun and K. Barta, *ACS Sustainable Chem. Eng.*, 2019, **7**, 11267–11274; (*i*) K. Zhou, H. Liu, H. Shu, S. Xiao, D. Guo, Y. Liu, Z. Wei and X. Li, *ChemCatChem*, 2019, **11**, 2649–2656; (*j*) C. R. Ho, V. Defalque, S. Zheng and A. T. Bell, *ACS Catal.*, 2019, **9**, 2931–2939.

7 (*a*) R. Pfützenreuter and M. Rose, *ChemCatChem*, 2016, **8**, 251–255; (*b*) D. Ruiz, A. Aho, T. Saloranta, K. Eränen, J. Wärnå, R. Lino and D. Y. Murzin, *Chem. Eng. J.*, 2017, **307**, 739–749; (*c*) D. Ruiz, A. Aho, P. Mäki-Arvela, N. Kumar, H. Oliva and D. Y. Murzin, *Ind. Eng. Chem. Res.*, 2017, **56**, 12878–12887; (*d*) Y. Li, H. Chen, C. Zhang, B. Zhang, T. Liu, Q. Wu, X. Su, W. Lin and F. Zhao, *Sci. China Chem.*, 2017, **60**, 920–926; (*e*) G. Liang, Y. Zhou, J. Zhao, A. Y. Khodakov and V. V. Ordomsky, *ACS Catal.*, 2018, **8**, 11226–11234.

8 (*a*) A. K. Rausch, E. van Steen and F. Roessner, *J. Catal.*, 2008, **253**, 111–118; (*b*) J. H. Cho, J. H. Park, T.-S. Chang, G. Seo and C.-H. Shin, *Appl. Catal. A; Gen.*, 2012, **417–418**, 313–319; (*c*) F. Niu, S. Xie, M. Bahri, O. Ersen, Z. Yan, B. T. Kusema, M. Pera-Titus, A. Y. Khodakov and V. V. Ordomsky, *ACS Catal.*, 2019, **9**, 5986–5997.

9 T. Tong, W. Guo, X. Liu, Y. Guo, C.-W. Pao, J.-L. Chen, Y. Hu and Y. Wang, *J. Catal.*, 2019, **378**, 392–401.

10 (*a*) C. Copéret, D. P. Estes, K. Larmier and K. Searles, *Chem. Rev.*, 2016, **116**, 8463–8505; (*b*) F. Polo-Garzon, S. Luo, Y. Cheng, K. L. Page, A. J. Ramirez-Cuesta, P. F. Britt and Z. Wu, *ChemSusChem*, 2018, **12**, 93–103.

11 (*a*) K. Motokura, N. Fujita, K. Mori, T. Mizugaki, K. Ebitani, K. Jitsukawa and K. Kaneda, *Chem. -Eur. J.*, 2006, **12**, 8228–8239; (*b*) K. Motokura, D. Nishimura, K. Mori, T. Mizugaki, K. Ebitani and K. Kaneda, *J. Am. Chem. Soc.*, 2004, **126**, 5662–5663.

12 G. Delleplane and J. Overend, *Spectrochim. Acta*, 1966, **22**, 593–614.

13 S. Y. Chin, C. T. Williams and M. D. Amiridis, *J. Phys. Chem. B*, 2006, **110**, 871–882.

14 T. Komanoya, T. Kinemura, Y. Kita, K. Kamata and M. Hara, *J. Am. Chem. Soc.*, 2017, **139**, 11493–11499.

15 I. Delidovich, P. J. C. Hausoul, L. Deng, R. Pfützenreuter, M. Rose and R. Palkovits, *Chem. Rev.*, 2016, **116**, 1540–1599.

16 (*a*) N.-T. Le, A. Byun, Y. Han, K.-I. Lee and H. Kim, *Green Sustainable Chem*, 2015, **5**, 115–127; (*b*) K. Zhou, H. Liu, H. Shu, S. Xiao, D. Guo, Y. Liu, Z. Wei and X. Li, *ChemCatChem*, 2019, **11**, 2649–2656; (*c*) H. Yuan, B. T. Kusema, Z. Yan, S. Streiff and F. Shi, *RSC Adv.*, 2019, **9**, 38877–38881.

17 Y. Kim, S. Ahn, J. Y. Hwang, D.-H. Ko and K.-Y. Kwon, *Catalysts*, 2017, **7**, 7.

18 X. Xue, J. Liu, D. Rao, S. Xu, W. Bing, B. Wang, S. He and M. Wei, *Catal. Sci. Technol.*, 2017, **7**, 650–657.

19 M. I. Zaki, M. A. Hasan, F. A. Al-Sagheer and L. Pasupulety, *Langmuir*, 2000, **16**, 430–436.

20 H. D. Kaesz and R. B. Saillant, *Chem. Rev.*, 1972, **72**, 231–281.

21 K. Aika, A. Ohya, A. Ozaki, Y. Inoue and I. Yasumori, *J. Catal.*, 1985, **92**, 305–311.